JOURNAL OF AIRCRAFT
Vol. 47, No. 3, May–June 2010

Propulsion and Flight Controls Integration for a Blended-Wing-Body Transport Aircraft

Naveed U. Rahman* and James F. Whidborne†
Cranfield University, Bedfordshire, England MK43 0AL, United Kingdom

DOI: 10.2514/1.46195

While operating at low airspeeds with nominal static margins, the controls on a blended-wing-body aircraft begin to saturate, and the dynamic performance gets sluggish. Augmentation of aerodynamic controls with the propulsion system is therefore considered in this research. Two aspects were of interest: namely, thrust vectoring and flap blowing. An aerodynamic model for a large blended-wing-body transport aircraft with blown flap effects was formulated using empirical and vortex lattice methods and then integrated with a Trent 500 turbofan engine model. To enhance control effectiveness, both internally and externally blown flaps were simulated. For a full-span internally blown flap arrangement using intermediate compressor flow, the amount of engine bleed and the resulting blowing coefficients were limited. However, even with a reduced bleed mass flow, the pitch control effectiveness increases by 15.9% at 85% fan revolutions per minute. For an externally blown flap arrangement using bypass air, much higher blowing coefficients can be achieved. For instance, at 100% fan revolutions per minute, there is a 44% increase in pitch control authority at low dynamic pressures. The main benefit occurs during takeoff, where both thrust vectoring and flap blowing help in achieving early pitch rotation, reducing takeoff field length and liftoff speed considerably. With central flap blowing and a limited thrust vectoring of 10°, the liftoff range reduces by 48%, and liftoff speed reduces by almost 26%.

Nomenclature

A_{jet}	=	wing nozzle, exit area
C_L, C_D, C_m	=	lift, drag, and pitch moment coefficient
C_u	=	blowing momentum coefficient
M_a	=	aerodynamic pitching moment about c.g.
M_{LG}	=	pitching moment about main landing gear
$\dot{m}_{\text{jet}}$	=	wing nozzle, jet mass flow
$\bar{q}$	=	dynamic pressure
V_{jet}	=	wing nozzle, jet velocity
x/l	=	bleed location (x) along compressor length (l)
X_a, X_g, X_E	=	X-body axis aero, gravity, and thrust forces
Z_a, Z_g, Z_E	=	Z-body axis aero, gravity, and thrust forces
α, β	=	angle of attack and sideslip
δ_a, δ_e, δ_T	=	aileron, elevator, and throttle position

I. Introduction

THE flying wing design is potentially an attractive configuration due to the aerodynamic performance advantages it offers over its conventional counterpart [1]. However, the omission of horizontal and vertical stabilizers leads to stability and control authority issues. The blended-wing body (BWB) is a special kind of tailless aircraft that has gained renewed interest despite these stability and control deficiencies. The following are some of the potential benefits of the aircraft:

1) Absence of a tail and a fuselage implies lesser wetted area and, therefore, less drag. From the aerodynamics point of view, this means lesser power is required at cruise condition and, therefore, potentially fewer engines for the same payload. For an environmental perspective, it means lower emissions per passenger or a greener aircraft.

2) Low landing speeds are desirable for all types of aircraft. In the BWB concept, the fuselage also produces a significant amount of lift in addition to the outboard wings. Therefore, at low airspeeds, it might not be necessary to use high-lift devices, which add weight and complexity into the system.

3) Another concept that has been gaining interest is to mount the engines above the fuselage reference line (FRL). The blended fuselage will then act as a noise shield, reflecting most of the energy away from ground. This has led to the Silent Aircraft Initiative [2], a joint project undertaken by the Massachusetts Institute of Technology and Cambridge University. Although still in its infancy, use of thrust vector control (TVC) is already being considered for the pitch axis [3].

Despite these, the BWB concept has many technical challenges, such as 1) optimization of the planform for a higher lift-to-drag ratio than conventional configurations, 2) structural design of a noncylindrical pressurized fuselage, 3) provision of adequate stability and control authority over the full flight envelope, and 4) a low-emission/low-noise propulsion system. This research, however, focuses just on the stability and control aspects and evaluates if they can be modified/improved by means of the propulsion system.

The use of a propulsion system to augment aerodynamic controls extends the role of the propulsion system beyond that of provision of thrust to sustain flight. The research methodology was therefore set so as to model both the aerodynamics and the propulsion system as accurately as possible and achieve optimum controls performance without compromising the efficiency of the propulsion system. In this context, both jet/blown flaps and TVC were evaluated:

1) For jet flaps, if a certain amount of air from a pressure source (such as the engine compressor) is blown onto the upper trailing edge of the aerodynamic control surface (as shown in Fig. 1), it reenergizes the boundary layer, and both the lift curve slope and flap effectiveness increase [4]. Explanations of the effect can be found in several sources [5,6]. Englar et al. [7,8] states that this concept has the potential of generating lift comparable to that of the mechanically complex high-lift configurations. In fact, Englar et al. [7,8] dispensed with the conventional controls completely in favor of differential blowing for control on all three axes for a Boeing B737-100.

2) For thrust vector control, an alternate method for control augmentation is the use of vectored thrust by limited deflection of the exhaust jet. TVC provides an additional control force but with a corresponding loss in the net axial thrust.

This research considers some aspects of flight controls and propulsion systems integration for a large transport BWB aircraft [9,10]. The aircraft is summarized in the next section. The previous

Received 30 June 2009; revision received 5 December 2009; accepted for publication 28 February 2010.

*Research Student, Dynamics, Simulation and Controls Group.
†Ph.D., Chartered Engineer, Dynamics, Simulation and Controls Group.

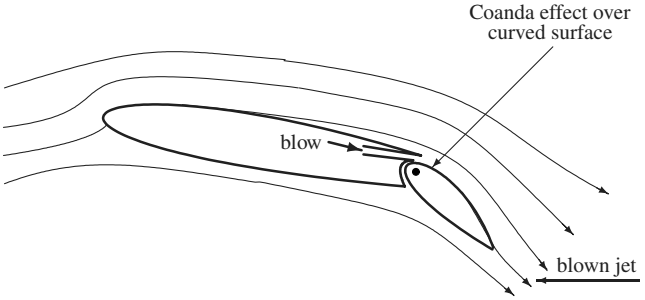

Fig. 1 Flow control through a trailing-edge blown flap [5,6].

study of this aircraft [9] showed that the lack of a tailplane and resulting low moment arms means that the aircraft has some deficiencies in terms of the handling and flying qualities. The aim of this work is to determine the potential for these deficiencies to be rectified by use of the propulsion system, using jet flaps and TVC, and to determine the resulting effect on the propulsion system. It should be noted that this work is not intended to provide a definitive statement on the subject, as there are a number of important engineering considerations that have not been considered at all in this paper. Basic integration of the propulsion system with the airframe in itself is a complex process, involving many aspects such as the fuel system integration, engine system monitoring and control, engine weight, noise and c.g. considerations, etc. However, when the role of the propulsion system is extended beyond that of provision of thrust to that of controls augmentation, a number of additional aspects must also be considered; these include: 1) the weight of the ducting if internally blown flaps are used, 2) the ducting arrangement, 3) effects of hot gas impingement on the control surfaces and ducts themselves, and 4) the increase in structural complexity and resulting difficulties with manufacture and maintainability.

This work included the development of a turbofan engine model and a BWB aircraft model with blown flaps. The purpose of the engine modeling effort was to evaluate the effects of engine bleed and vectored thrust on engine performance. This engine model is covered in detail in [11]. The BWB aerodynamic model with blown flap effects was formulated using empirical and vortex lattice methods [12] and is discussed in the next section.

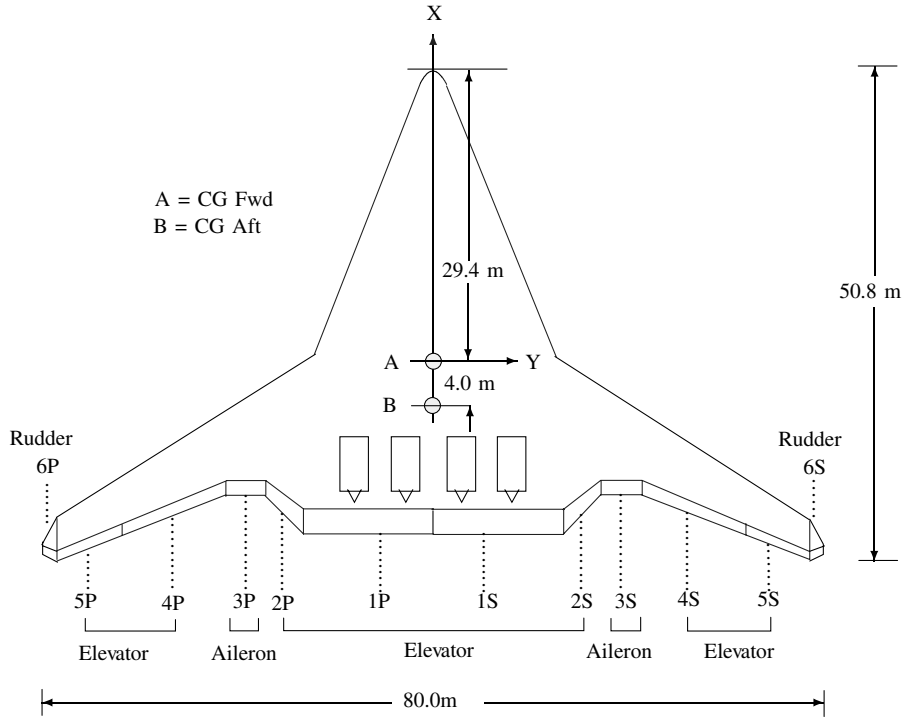

Fig. 2 BWB transport aircraft general layout [9,10].

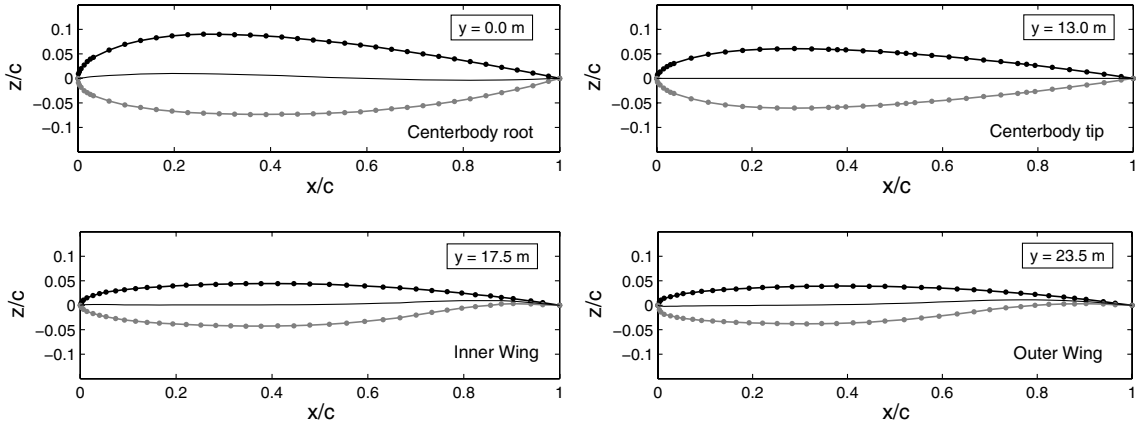

Fig. 3 BWB wing sections: centerbody and inner and outer profiles [10].

II. Blended-Wing Body Aircraft Model with Blown Flaps

A. Blended-Wing Body Model Formulation

This research considers the flight controls and propulsion systems integration for a large transport BWB aircraft. The planform shape and the airfoil profiles have been obtained from Castro [9] and Qin et al. [10]. A general layout of the aircraft is shown in Fig. 2. The aircraft has a span of 80 m and has 12 control surfaces numbered from left to right. Two of these surfaces, 6S (starboard) and 6P (port), are on the vertical fins and provide the rudder function. The remaining 10 control surfaces are located on the trailing edge of the lifting body and provide for lateral (roll) and longitudinal (pitch) control functions. A maximum takeoff weight of 371,280 kg was assumed, whereas the maximum landing weight was set at 322,599 kg. The c.g. variation is from 29.4 to 33.4 m, with the neutral point being at approximately 31.6 m. Design point cruise is at Mach 0.85 at an altitude 10,059 m and the landing speed is between 150–160 kt.

The BWB planform considered in this work had variable twist along the span and different sweep back angles for the inboard and outboard wing sections. In addition, it had an aerodynamic camber section profile that varied from reflexed camber for the inboard sections, nearly symmetric for the midspan and supercritical for the outboard wing (see Fig. 3). This made the aerodynamic estimation problem complicated, so a strip element model for this aircraft was built so that the contribution of each strip to lift drag and pitching moment could be individually calculated. Extensive use of Engineering Sciences Data Units (ESDU) was made to develop this airframe model. The model was then validated against the available [9]. The effect of flap blowing was incorporated using the jet-flap theory as illustrated by Spence [4] and Williams et al. [13].

Figure 4 shows two strip elements (1 and 2) with the elemental body axis forces acting ahead and behind the c.g., respectively. For point 1, an upward Z force generates a positive pitching moment and negative rolling moment. Similarly, for point 2, an upward Z force generates a negative pitching moment and a negative rolling moment. The elemental lift and drag forces $[L_y, D_y]$, when converted to body axis, generate elemental $[X_y, Y_y, Z_y]$ forces in the body axis as

$$\begin{bmatrix} X_y \\ Y_y \\ Z_y \end{bmatrix}_{\text{body}} = \begin{bmatrix} \cos\alpha\cos\beta & -\cos\alpha\sin\beta & -\sin\alpha \\ \sin\beta & \cos\beta & 0 \\ \sin\alpha\cos\beta & -\sin\alpha\sin\beta & \cos\alpha \end{bmatrix} \begin{bmatrix} -D_y \\ 0 \\ -L_y \end{bmatrix}_{\text{wind}} \tag{1}$$

Each of these forces can be summed up to generate the net X, Y, and Z forces in the body axis due to the wing alone.

Similarly, the sectional pitching moment about the quarter-chord point is transformed from wind to body axis to get $[L_y, M_y, N_y]$. The net moments about the c.g. can then be calculated as

$$\begin{bmatrix} L \\ M \\ N \end{bmatrix}_{\text{cg}} = \sum^{1:n} \begin{bmatrix} L_y + Z_y y \\ M_y - Z_y x \\ N_y - X_y y + Y_y x \end{bmatrix} \tag{2}$$

where the distance x is defined as $(x_{\text{cg}} - x_{\text{pos}_{c/4}})$ and is positive toward the nose, y is the lateral distance of the strip from the centerline positive starboard, and n is the number of strips.

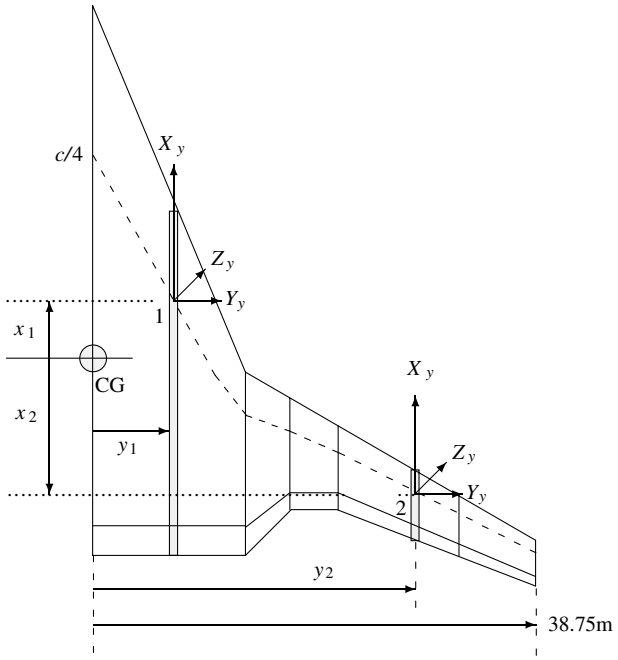

Fig. 4 Forces and moments on the BWB wing.

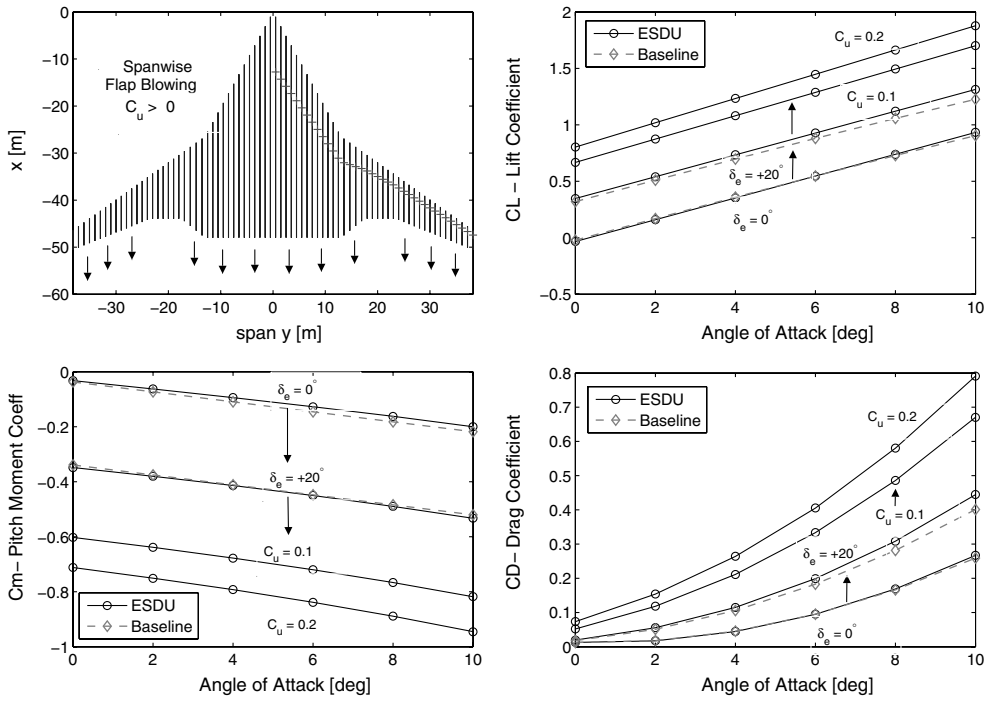

Fig. 5 Model validation and effect of blown flaps 1, 2, 4, and 5 (pitch axis).

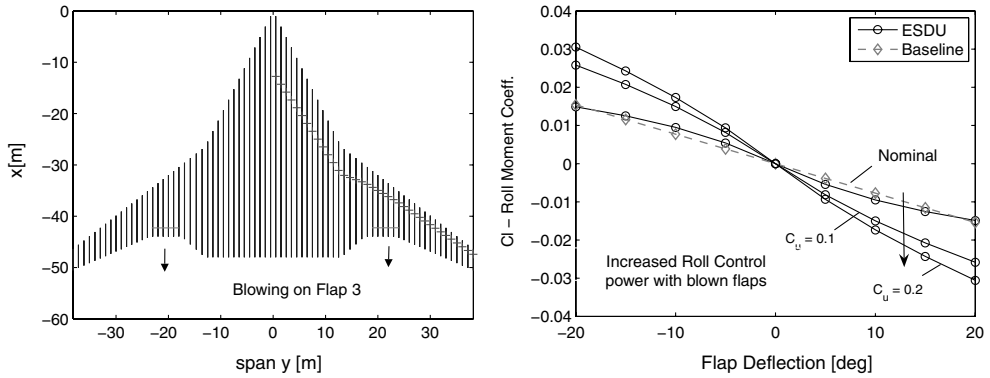

Fig. 6 Model validation and effect of blown flap 3 (roll axis).

1. Lift Estimates with Blowing

The sectional lift coefficient with blown flap effects included is

$$[C_L]_y = [C_{L0_B} + \Delta C_{L0_{\text{flap}}} + \Delta C_{L0_{C_u}}]_y + K_1 C_{L_\alpha}(\alpha_y + \Delta\alpha_\Gamma + \Delta\alpha_{\text{twist}}) \tag{3}$$

where C_{L0_B} is the basic lift coefficient at zero α for a clean airfoil, $\Delta C_{L0_{\text{flap}}}$ is the change in lift coefficient due to flap deflection, and $\Delta C_{L0_{C_u}}$ is the increment in lift coefficient for a blown flap. This increment is based on experimental results by Williams et al. [13] and is also verified theoretically by Spence [4]. For a two-dimensional section,

$$\Delta C_{L0_{C_u}} = C_{L_\delta}\delta \tag{4}$$

$$C_{L_\delta} = [4\pi C_u(1 + 0.151C_u^{1/2} + 0.139C_u)]^{1/2} \tag{5}$$

where δ is the flap deflection. In Eq. (3), factor K_1 is incorporated to simulate the effect of increase in lift curve slope with blowing. Williams et al. [13] suggests that K_1 is approximated by

$$K_1 = (1.0 + 0.151C_u^{1/2} + 0.219C_u) \tag{6}$$

The effective angle of attack α_y for each strip along the span is modified by local dihedral Γ_y on account of sideslip ($\Delta\alpha_\Gamma = \beta\Gamma$) and the sectional twist $\Delta\alpha_{\text{twist}}$. Both wing sweep and taper induce a

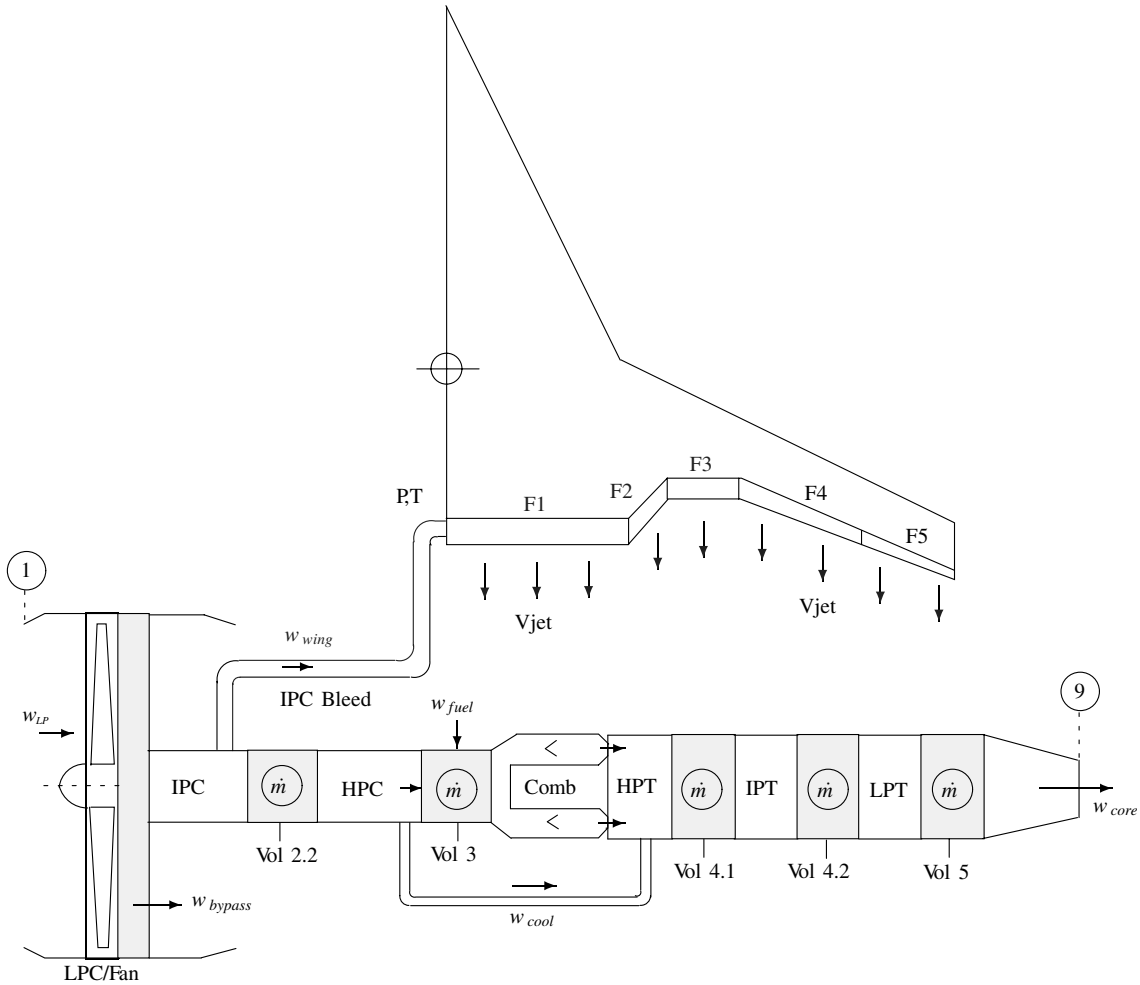

Fig. 7 BWB Aircraft with IPC bleed for internally blown flaps. (LPC: low-pressure compressor, HPC: high-pressure compressor, LPT: low-pressure turbine, IPT: intermediate-pressure turbine, HPT: high-pressure turbine).

spanwise downwash, which modifies the effective angle of attack, as seen by an airfoil section along the span. This variation in the spanwise angle of attack due to three-dimensional effects was estimated using a vortex lattice/panel code, TORNADO [12], and incorporated in Eq. (3) to obtain a corrected spanwise lift distribution.

2. Drag Estimates

The sectional drag coefficient was calculated as a sum of two parts: 1) the profile drag coefficient C_{D_0}, and 2) the drag due to lift or vortex drag C_{D_v}. Thus,

$$[C_D]_y = C_{D_0} + C_{D_v} = C_{D_{0B}} + \Delta C_{D_{0\text{flap}}} + KC_L^2 \tag{7}$$

where $C_{D_{0B}}$ is the profile drag coefficient of a clean airfoil, and the increment in profile drag due to flap deflection is given by $\Delta C_{D_{0\text{flap}}}$ and is a function of flap chord length and flap deflection. The lift-dependent drag term K was approximated using the drag polar obtained from [14] computational fluid dynamics runs.

3. Pitch Moment Estimates

The sectional pitching moment coefficient about the quarter-chord position was calculated as

$$[C_{m_{c/4}}]_y = [C_{m0i}]_{c/4} + [\Delta C_{m0}]_{\text{flap}} - (C_L - C_{L0_B})h_1 \tag{8}$$

where $[C_{m0i}]_{c/4}$ is the pitching moment about the quarter-chord position for a clean airfoil at zero α, $[\Delta C_{m0}]_{\text{flap}}$ is the increment in pitching moment at zero α due to the deflection of a plain trailing-edge flap, and h_1 is the location of center of lift due to angle of attack and flap deployment, aft of the $c/4$ position.

B. Model Validation and Effect of Blown Flaps

1. Lift, Drag, and Pitching Moment: (C_L, C_D, C_m)

Figure 5 shows the net lift, drag, and pitching moment coefficients at a blowing coefficient (C_u) of 0.1 and 0.2, respectively. A constant flap deflection of $+20°$ is assumed on all flaps except flap 3, which is used as an aileron. Two points can be noted from Fig. 5: 1) the lift coefficient C_L increases with an increase in blowing coefficient, and 2) the negative increment in pitching moment due to flap blowing is significant. Also shown for comparison are the results of the baseline BWB aircraft from [9] for the unblown flap case.

2. Rolling Moment: (C_l)

Figure 6 shows a comparison of roll control powers for the baseline [9] and the ESDU models for the inboard aileron (flap 3). The increase in roll power with blown flaps is indicated. The control power almost doubles for a blowing coefficient of 0.2. As elaborated later, this proves to be of great advantage in achieving better/faster roll performance at landing and takeoff speeds.

III. Results: Propulsion and Flight Controls Integration

As discussed in the previous section, the lift and pitching moment characteristics for the BWB can be modified by use of blown flaps. The source of bleed air can either be the low-pressure (LP), the intermediate-pressure (IP) or the high-pressure (HP) compressor, depending upon the wing duct pressure requirements. However, for the three-spool turbofan considered, 20% of the HP mass flow is already used for HP turbine cooling, and the wing nozzle pressure requirements for flap blowing purposes are usually less; it was therefore decided not to bleed the HP stage further, and only the IP and LP stages are considered for flap blowing.

A. Internally Blown Flap Arrangement Using Intermediate-Pressure Compressor Bleed

Figure 7 shows bleed offtake from the IP compressor (IPC) in an internally blown flap arrangement. In this case, the blowing coefficient C_u will be determined by 1) the slot height that sets the actual wing nozzle exit area, 2) the bleed offtake location along compressor length, which sets the total pressure and temperature $[P, T]$ of the source reservoir in combination with the throttle setting, and 3) the dynamic pressure. To see the effect of slot height on the stripwise blowing coefficient, $[C_u]_y$, consider

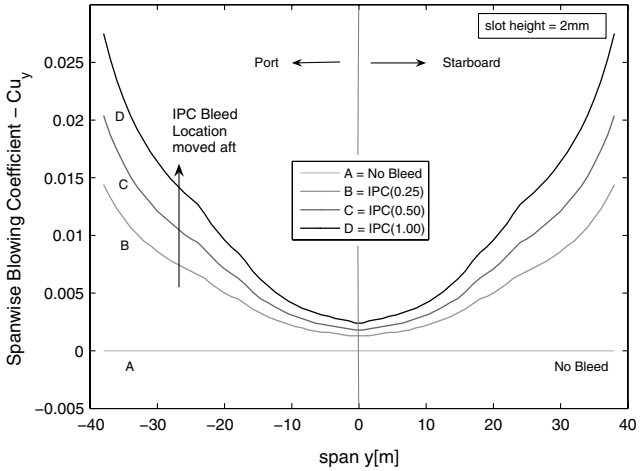

Fig. 8 Variation in spanwise blowing coefficient with IPC bleed location or increasing $[P, T]$.

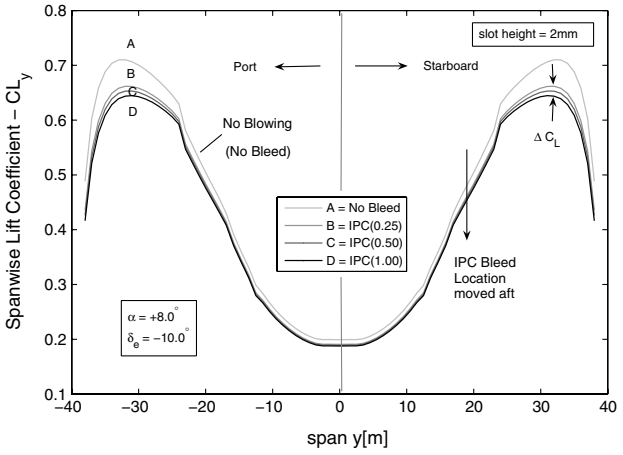

Fig. 9 Variation in spanwise lift coefficient with IPC bleed location or increasing $[P, T]$.

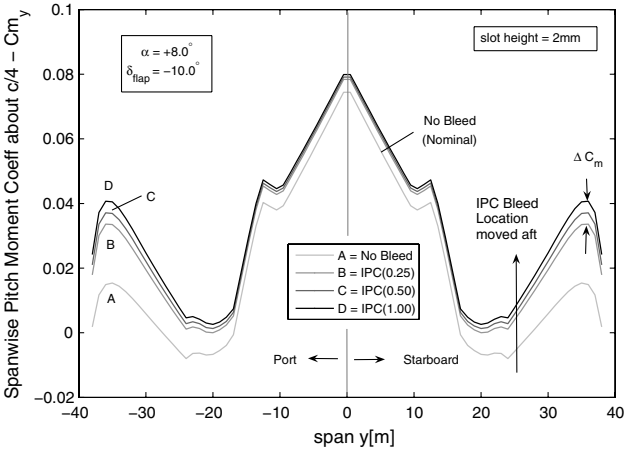

Fig. 10 Variation in spanwise pitching moment coefficient with IPC bleed location or increasing $[P, T]$.

Table 1 Engine/airframe parameters and IPC bleed location at 85% throttle (TET denotes turbine entry temperature.)

Case	Bleed loc., (x/l)	ΔTET, K	$P_{2.2}$, atm	$T_{2.2}$, K	$\dot{m}_{\text{jet}}$, kg/s	V_{jet}, m/s	C_u, average	$\Delta C_L/\Delta_{\text{flap}}$, relative	$\Delta C_m/\Delta_{\text{flap}}$, relative
A	No bleed	——	——	——	——	——	0.0000	1.000	1.000
B	0.25	+39	2.58	371	21.1	352	0.0057	1.092	1.116
C	0.50	+100	3.52	418	27.1	374	0.0078	1.107	1.135
B	1.00	+241	4.71	495	33.4	407	0.0103	1.119	1.159

$$[C_u]_y = \frac{\dot{m}_{\text{jet}} V_{\text{jet}}}{\bar{q} S_y} = \frac{(\rho_{\text{jet}} A_{\text{jet}} V_{\text{jet}}) V_{\text{jet}}}{\bar{q} S_y} = \frac{\rho_{\text{jet}} w h V_{\text{jet}}^2}{\bar{q} w c_y} = \frac{\rho_{\text{jet}} h V_{\text{jet}}^2}{\bar{q} c_y} \quad (9)$$

where $\dot{m}_{\text{jet}}$ is the exiting mass flow for each strip, V_{jet} is the jet velocity, $\bar{q}$ is the freestream dynamic pressure, and S_y is the local strip area. Also, $\dot{m}_{\text{jet}} = \rho_{\text{jet}} A_{\text{jet}} V_{\text{jet}}$, $A_{\text{jet}} = wh$, and $S_y = wc_y$, where w is the strip or slot width and h is the slot height. In Eq. (9), for a constant slot height h, the spanwise blowing momentum coefficient varies with local chord c_y. For the following analysis, a constant slot height of $h = 2$ mm is assumed along with a throttle setting of 85% and an airspeed of 200 kt.

Figure 8 shows the spanwise blowing momentum coefficient and the effect of IPC bleed offtake location. The curve marked as B represents the IPC $(x/l = 0.25)$ bleed case, where x/l is the nondimensional bleed location along compressor length. Cases C and D represent IPC(0.5) and IPC(1.0), respectively. As the bleed location is moved aft (end of IPC), the jet mass flow $\dot{m}_{\text{jet}}$ and velocity V_{jet} increase and, therefore, the blowing momentum coefficient.

Figure 9 shows the corresponding spanwise lift coefficient. On Fig. 9, the lift curves for 2 mm slot height and bleed locations of IPC (1.0), IPC(0.5), and IPC (0.25) are grouped quite close together and the change ΔC_L is relatively small. This indicates that even at smaller blowing coefficients of IPC(0.25) or IPC(0.5), significant changes in flap effectiveness can be achieved with much lower penalties on engine performance. Since the flap/elevator deflection is assumed negative ($\delta_{\text{flap}} = -10°$) as required for pitch trim at low speeds, the effect of flap blowing appears as a greater increase in the flap effectiveness ($\Delta C_L/\Delta_{\text{flap}}$).

Figure 10 shows the spanwise pitching moment about sectional $c/4$ positions for the ESDU model at a flap deflection of $\delta_{\text{flap}} = -10°$ and $\alpha = +8°$. From Fig. 10, the spanwise pitching moment is positive for the centerbody section relative to the outboard wing sections. This is due to the reflexed cambered airfoil for the centerbody, and it is vital for pitch trim and reduction in trim elevator

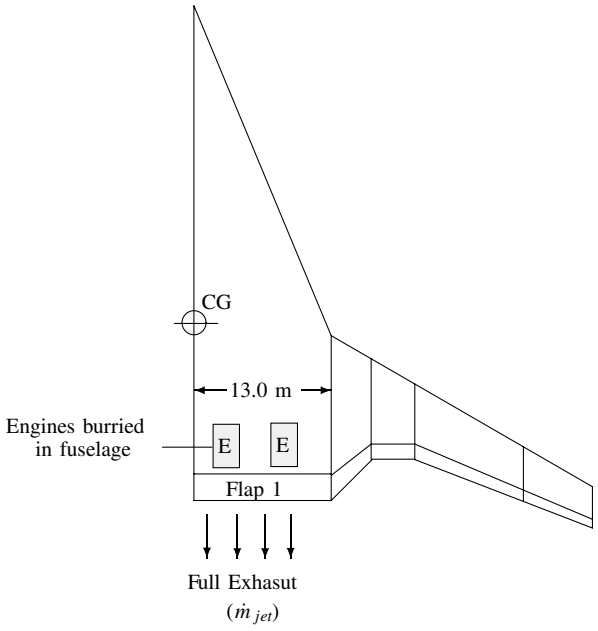

Fig. 11 Flap 1 in a fully blown external flap arrangement.

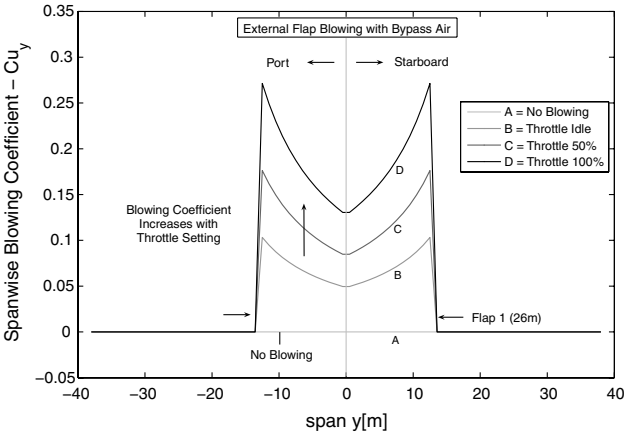

Fig. 12 Spanwise blowing coefficient: externally blown centerbody flap.

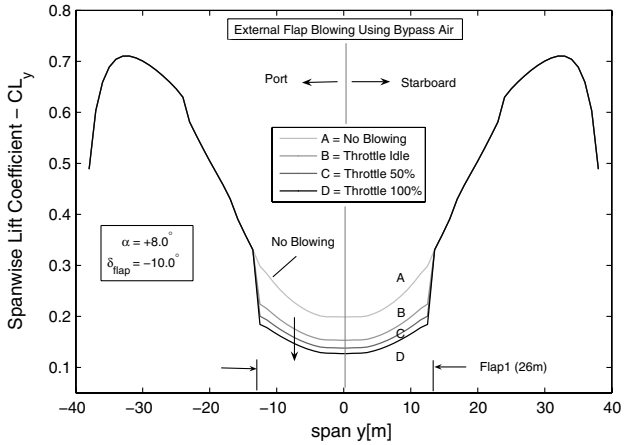

Fig. 13 Spanwise lift coefficient: externally blown centerbody flap.

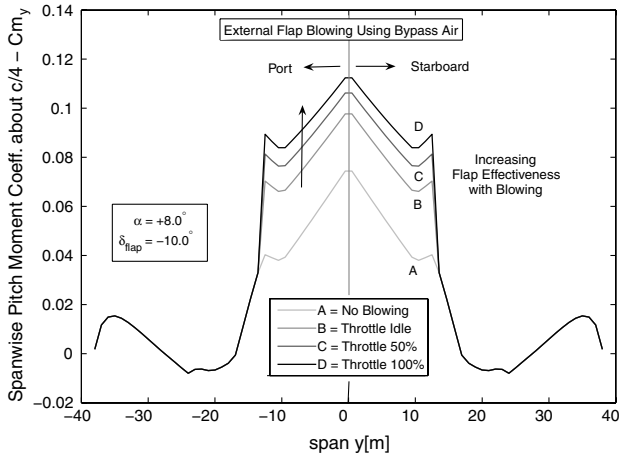

Fig. 14 Spanwise pitch moment coefficient: externally blown centerbody flap.

Table 2 Externally blown centerbody flaps using bypass flow (B = bypass, C = core)

Case	Throttle	Thrust, kN	B flow, kg/s	C flow, kg/s	B vel., m/s	C vel., m/s	$[C_u]_{F1}$, average	$\Delta C_L/\Delta_{\text{flap}}$, relative	$\Delta C_m/\Delta_{\text{flap}}$, relative
A	Idle	——	——	——	——	——	0	1.000	1.000
B	Idle	47.5	523.4	54.8	182.0	220.0	0.0734	1.248	1.264
C	50%	116.0	683.4	88.6	238.7	386.2	0.1262	1.317	1.352
D	100%	238.5	840.5	135.1	297.2	567.8	0.1930	1.385	1.442

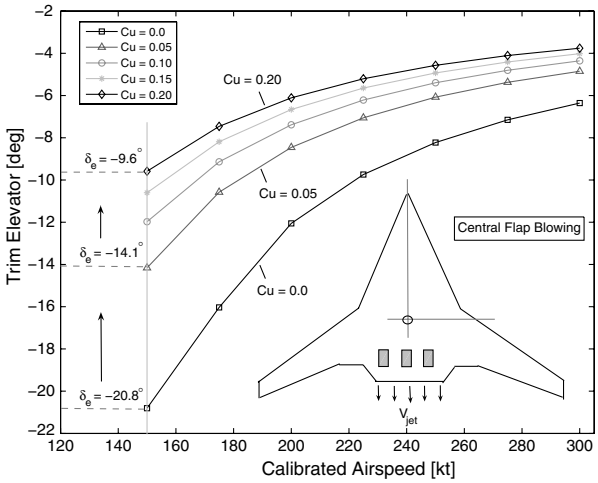

Fig. 15 Trim results: aerodynamic flight control and central flap blowing, trim elevator, $x_{cg} = 29.4$ m, level flight.

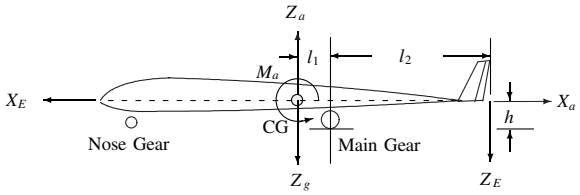

Fig. 16 Forces and moments on the BWB during takeoff.

deflections for a tailless design. The effect of blown flaps appears as greater increase in positive pitching moment when flaps are deflected negative, as marked by the positive shift in curves B, C and D. Table 1 summarizes these results.

For the three-spool turbofan considered, IPC bleed locations from 0.25 to 0.50 are enough to sustain high jet velocities (374 to 352 m/s) and mass flows (27.1 to 21.1 kg/s) per engine. The average blowing coefficient is reduced from 0.0103 to 0.0057; however, the relative flap effectiveness is still 11.6% higher than the unblown case.

B. Externally Blown Flaps Using Bypass/Main Flow

The bleed mass flow from the LP compressor/fan stage can either be blown over the full span, as in the case of a distributed propulsion concept, or the full exhaust, including the bypass, and the core mass flow can be blown over selected flaps directly, without the need for internal wing ducting. For the BWB, many researchers are already proposing to embed the engines within the fuselage to enhance noise shielding [15]. This means that the engine's vertical offset from the FRL would be small, and it is theoretically possible to place a rectangular engine exhaust just before the trailing-edge flap, specifically flap 1, which has a span of 26 m. This will result in an externally blown flap arrangement. Such a configuration is shown in Fig. 11.

Figure 12 shows the increase in blowing coefficient for flap 1 due to external flap blowing. At 100% throttle setting and using a 4×275 kN Trent 500 engine configuration, the average value of C_u for flap 1 is 0.2. This may seem to be a bit low, keeping in view that full bypass air is blown over the flaps; however, the local chords for the centerbody are unusually large (48 m for the root section) which makes it difficult to achieve high blowing coefficients. In addition, flap 1 has a length of 26 m, which reduces the mass flow per unit span.

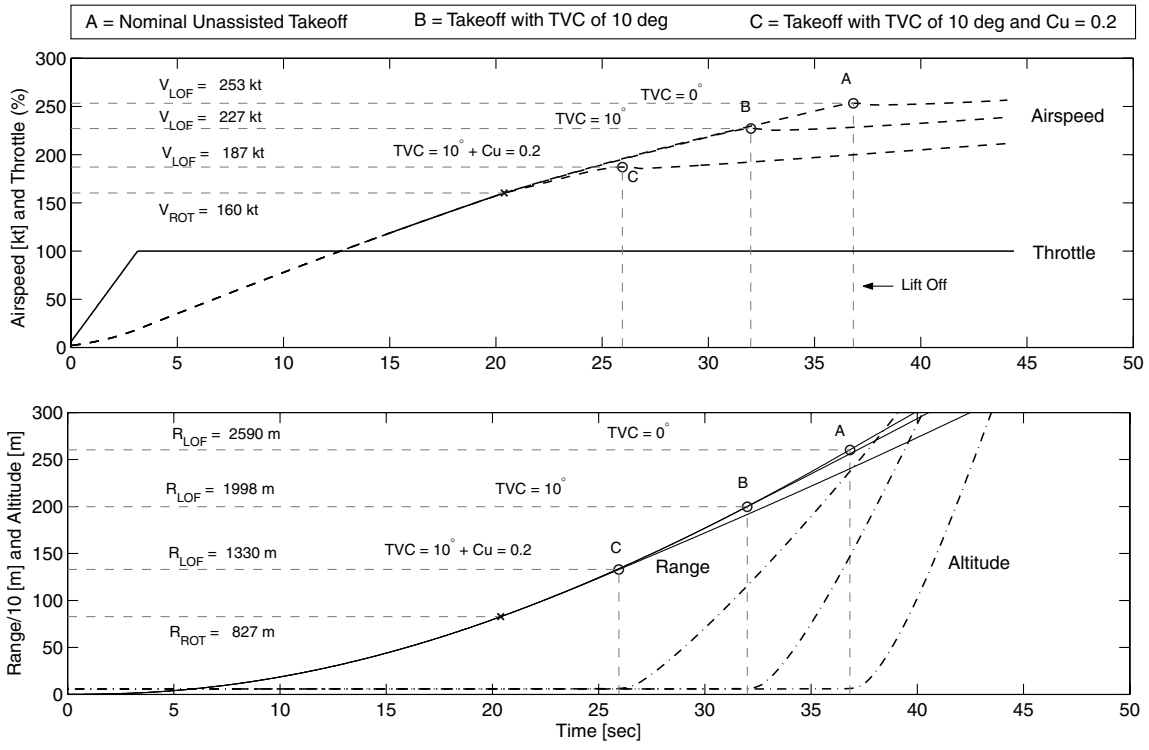

Fig. 17 Takeoff performance with limited TVC and flap blowing.

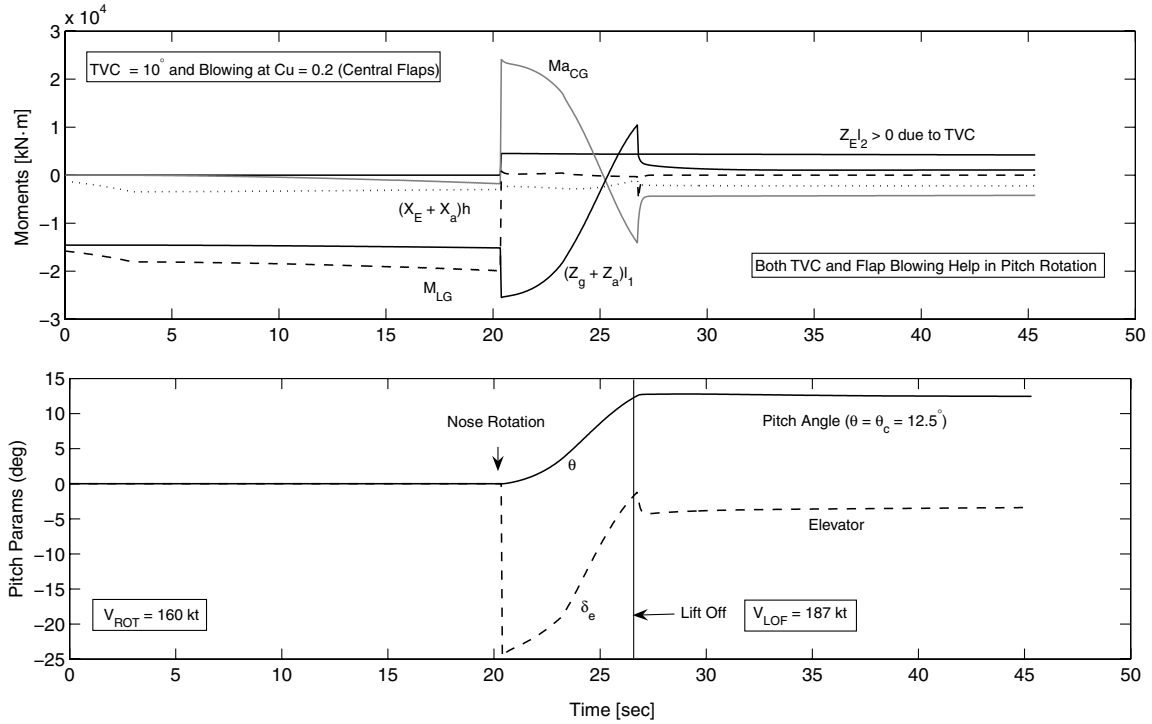

Fig. 18 Pitch moments about main landing gear with TVC and blown flaps.

Figure 13 shows the corresponding spanwise lift coefficient for $\alpha = +8°$ and spanwise flap deflection of $-10°$. The increase in flap effectiveness due to blowing for the centerbody are marked by curves B, C and D for various throttle settings. Similar results can be seen for spanwise pitching moment coefficient on Fig. 14. Flap 1 is now more effective and the nose up pitching moment is greater than the unblown case.

The results have been summarized in Table 2. Even at idle throttle settings, the increase in flap effectiveness is +26.4% relative to the unblown case. At full throttle, this increases to +44.2%. It may be noted here that only the centerbody flaps are blown; the flap effectiveness is, however, considered for full span or the overall moment generated about the c.g. and not for individual flaps, which is considerably higher and is illustrated in Fig. 14. The reduction in trim elevator with externally blown flaps is shown in Fig. 15.

IV. Takeoff Performance with Thrust Vectoring and Flap Blowing

Figure 16 shows a BWB aircraft in takeoff run. During takeoff, additional forces come into play, such as ground friction and reaction. In addition, the pitch rotation takes place about the main landing gear and not the c.g.. This means the weight of the aircraft along the Z-body axis Z_g and the Z-axis aerodynamic force Z_a also exert a moment about the landing gear. The distance of the c.g. from the main landing gear l_1 thus becomes an important consideration. The pitching moment equation used for takeoff analysis is listed below. Note that the reaction force from the nose landing gear has been neglected:

$$M_{\mathrm{LG}} = M_a - (Z_a + Z_g)l_1 - (X_a + X_E)h + Z_E l_2 \qquad (10)$$

In Eq. (10), M_a represents the aerodynamic moments about the c. g., including the blown flap effects, and the term $Z_E l_2$ is the pitching moment due to vectored thrust. For takeoff analysis, l_1 was set at 4.0 m, l_2 was set at 16.0 m, and the perpendicular distance of the thrust line from main landing gear (h) was set at 3.0 m. The nose wheel pitch setting angle was zero, and it is assumed that there is no ground effect.

Figure 17 shows the results of TVC of 10° and flap blowing on the centerbody at C_u of 0.2. The unassisted takeoff occurs at liftoff range of 2590 m and liftoff speed of 253 kt. With 10° of TVC, this reduces to 1998 m and 227 kt, respectively. Using external flap blowing on central flaps, with $C_u = 0.2$ in addition to 10° of TVC, the liftoff speed reduces to 187 kt and the range to 1330 m. These results could be better explained by a review of the pitching moment distribution about the main landing gear (Fig. 18).

With reference to Fig. 18, the pitching moment due to vectored thrust ($Z_E l_2$) is positive and corresponds to a TVC angle of 10°. The effect of blown flaps appears in the form of increased aerodynamic pitch moment about the c.g. ($M_{a_{\mathrm{CG}}}$). This, in combination with the positive pitching moment from TVC, is enough to rotate the nose, even at an airspeed of 160 kt. Table 3 presents a summary.

V. Roll Performance with Blown Flaps at Low Airspeeds

Owing to the planform shape and the mass distribution about the longitudinal axis, the roll axis inertia for the BWB aircraft is higher than for the conventional configurations. This, in combination with a high value of roll damping from the wing, limits the maximum achievable rate of roll. Low-speed bank angle performance therefore becomes sluggish and is a problem for the BWB aircraft.

Whereas the Boeing 747 aircraft uses the outboard aileron in addition to the inboard (high speed) aileron to improve the low-speed bank angle performance [16], implementation of a similar strategy for the BWB aircraft means a further reduction in pitch control

Table 3 Takeoff performance with TVC and central flap blowing

No.	TVC	C_u	V_{ROT}, kt	R_{LOF}, m	ΔR_{LOF}, %	V_{LOF}, kt	ΔV_{LOF}, %
1	0	0	160	2590	0	253	0
2	10.0	0	160	1998	−22.86	227	−10.28
3	10.0	0.20	160	1330	−48.65	187	−26.10

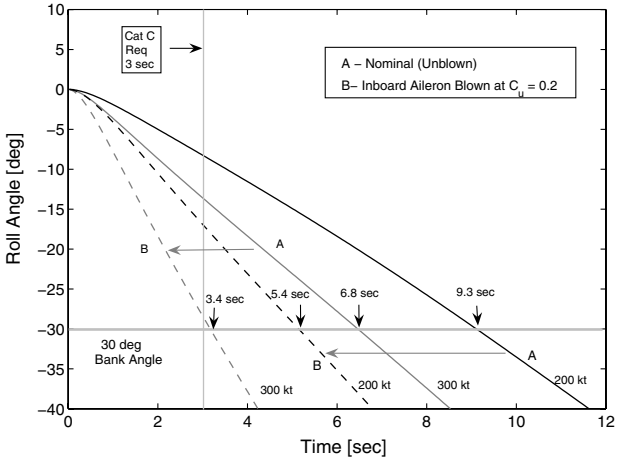

Fig. 19 Time to reach 30° bank angle, with and without flap blowing.

authority. An alternate option is, therefore, to enhance flap effectiveness of the aileron section using an internally blown flap arrangement.

Figure 19 shows the improvement in roll response obtained with an internally blown inboard aileron at a blowing coefficient of $C_u = 0.2$. The time to reach $-30°$ bank angle at a speed of 200 and 300 kt with full aileron deflection of $+25°$ is greatly improved and now almost meets the category C flight phase requirements for a large transport aircraft.

VI. Conclusions

Flap blowing causes a significant increase in flap effectiveness and therefore the pitching moment produced by it. However, bleed offtake from a compressor stage is expensive. With a 4×275 kN Trent 500 engine configuration, bleeding from the end of intermediate compressor IPC($x/l = 1.0$) at 85% fan revolutions per minute and a 2 mm full-span flap slot height causes almost 40% of IPC net mass flow to be bled and a significant degradation in engine performance. The resulting blowing coefficients were just below the critical value to prevent flow separation ($C_{u_{\text{crit}}} = 0.02$ to 0.03) and varied along the span with chord length. The degradation in engine performance can be avoided by either matching the engine for additional IPC bleed or bleeding the IPC at an earlier station along its axial length.

If the fan stage is used for external flap blowing, the fan exit/blowing pressure would be relatively less, and therefore the exit jet velocities will be low; however, there is theoretically no limit on the amount of mass flow that could be used for flap blowing. A feasible option is, therefore, to consider all of the bypass/core mass flow for external flap blowing on the centerbody section, which has a span of ± 13 m. Blowing coefficients in excess of 0.25 were shown to be easily achieved in this way. For the longitudinal axis, it is suggested to use external flap blowing directly, not only providing larger blowing coefficients but also a possible mechanism to deflect thrust.

The main benefit of augmentation of aerodynamic controls with the propulsion system occurs in the takeoff phase, where both TVC and flap blowing help in achieving early pitch rotation, thus reducing the takeoff field lengths and liftoff speeds considerably. Similarly for the roll axis, it was shown that control effectiveness can be enhanced if selected flaps, such as the inboard ailerons, are blown using an internally blown flap arrangement.

What has not been shown in this paper is the consequence of engine failure. Clearly, this is an important consideration for a vehicle relying on the propulsion systems for some of the controls. For the roll axis, it was shown that, at low airspeeds, the roll performance can be considerably improved by use of internally blown flaps. Some analysis of single-engine failures can be found in [17]. Upon onset of a single-engine failure, the roll performance would degrade in accordance with the reduction in the blowing momentum coefficient. However, for a two-engine failure condition, because of the degradation in the remaining operative engines resulting from the bleed, it is recommended not to use propulsion system augmentation but to fly on pure aerodynamic controls. For the pitch axis, a single-engine failure during the takeoff rotation phase would mean that a higher value of TVC/flap deflection shall be required to achieve the same takeoff length.

To conclude, it may be said that both flap blowing and TVC have comparable advantages in provision of additional control authority; however, there are a host of integration issues that would need to be considered before any conclusions could be made about the practical feasibility of this technology.

References

[1] Leibeck, R., "Design of the Blended Wing Body Subsonic Transport," *Journal of Aircraft*, Vol. 41, No. 1, 2004, pp. 10–25. doi:10.2514/1.9084

[2] Diedrich, A., Hileman, J., Tan, D., Wilcox, K., and Spakovsky, Z., "Multidisciplinary Design and Optimization of the Silent Aircraft," 44th AIAA Aerospace Sciences Meeting and Exhibit, AIAA Paper 2006-1323, 2006.

[3] Hileman, J. I., Reynolds, T. R., de la Rosa Blanco, E., and Law, T., "Development of Approach Procedures for Silent Aircraft," 45th AIAA Aerospace Sciences Meeting and Exhibit, AIAA Paper 2007-0456, 2007.

[4] Spence, D. A., "The Lift Coefficient of a Thin Jet-Flapped Wing," *Proceedings of the Royal Society of London*, Vol. 238, No. 1212, 1956, pp. 46–68. doi:10.1098/rspa.1956.0203

[5] Decken, J. V., "Aerodynamics of Pneumatic High Lift Devices," AGARD LS-43, 1970.

[6] Houghton, E. L., and Carpenter, P. W., *Aerodynamics for Engineering Students*, 5th ed., Butterworth–Heinemann, Oxford, 2003.

[7] Englar, R. J., Smith, M. J., Kelley, S. M., and Rover, R. C., "Application of Circulation Control to Advanced Subsonic Transport Aircraft, Part 1: Airfoil Development," *Journal of Aircraft*, Vol. 31, No. 5, 1994, pp. 1160–1168. doi:10.2514/3.56907

[8] Englar, R. J., Smith, M. J., Kelley, S. M., and Rover, R. C., "Application of Circulation Control to Advanced Subsonic Transport Aircraft, Part 2: Transport Application," *Journal of Aircraft*, Vol. 31, No. 5, 1994, pp. 1169–1177. doi:10.2514/3.46627

[9] Castro, H. V., "Flying and Handling Qualities of a Fly by Wire Blended Wing Body Civil Transport Aircraft," Ph.D. Thesis, Cranfield Univ., Bedfordshire, England, U.K., 2003.

[10] Qin, N., Vavalle, A., Le Moigne, A., Laban, M., Hackett. B., and Weinerfelt, P. "Aerodynamic Considerations of Blended Wing Body Aircraft," *Progress in Aerospace Sciences*, Vol. 40, No. 6, 2004, pp. 321–343. doi:10.1016/j.paerosci.2004.08.001

[11] Rahman, N. U., and Whidborne, J. F., "Real-Time Transient Three Spool Turbofan Engine Simulation: A Hybrid Approach, Transactions of the ASME," *Journal of Engineering for Gas Turbines and Power*, Vol. 131, No. 5, 2009, Paper 051602. doi:10.1115/1.3079611

[12] "User's Guide, Reference Manual, TORNADO 1.0," Royal Inst. of Technology, Stockholm, 2001.

[13] Williams, J. M., Butler, S. F., and Wood, M. N., "The Aerodynamics of Jet Flaps," Aeronautical Research Council Rept. 3304, London, Jan. 1961.

[14] "VGK Method for Two Dimensional Airfoil Sections Part 1: Principles and Results," IHS Engineering Sciences Data Units, ESDU 96028, London, April 2004.

[15] Agarwal, A., and Dowling, A., "A Ray Tracing Approach to Calculate Acoustic Shielding by the Silent Airframe," 44th AIAA Aerospace Sciences Meeting and Exhibit, AIAA Paper 2006-2618, 2006.

[16] Hefley, R. K., and Jewel, W. F., "Aircraft Handling Qualities Data," NASA, CR-2144, 1982.

[17] Rahman, N. U., "Propulsion and Flight Controls Integration for the Blended Wing Body Aircraft," Ph.D. Thesis, School of Engineering, Cranfield Univ., Bedfordshire, England, U.K., 2009.